Electron and ion emission in high-intensity laser irradiation of aluminum

Philippe Martin, Rusty Trainham, Pierre Agostini, and Guillaume Petite
Service de Recherche sur les Surfaces et l'Irradiation de la Matière, Centre d'Etudes de Saclay, 91191 Gif-sur-Yvette, France
(Received 10 July 1991)

Electron and ion emission from a laser-irradiated aluminum surface have been studied using time-of-flight spectrometry for laser intensities in the 10^6–10^9 W cm^{-2} range, at photon energies of 1.17, 2.34, or 3.51 eV and laser pulse durations varying from 29 to 150 ps. Both ion and electron emission were studied. Electron emission is found to dominate in the whole range of laser parameters explored, albeit by an amount that depends on the laser wavelength and pulse duration. Only singly charged ions are detected if one stays out of plasma conditions in front of the surface. We estimate an order of magnitude of the multiphoton-absorption probabilities using an inverse bremsstrahlung model on three different kinds of potentials (Yukawa, surface, and muffin-tin), and find that multiphoton absorption can almost certainly be understood using lowest-order perturbation theory. Fast electrons are detected, as in many other experiments of this kind, but we show that the spectrum broadening is symmetric, and probably due to transport effects. The dependence of the photocurrent on the different laser parameters is well explained using the Fowler-Dubridge theory of photoemission. Ion emission is found to have a "thermal" character, which is essentially governed by the laser fluence rather than the intensity.

I. INTRODUCTION

Electron emission from laser-irradiated surfaces has been studied almost since the laser came into existence. In most cases the photon energy is less than the sample's work function, so that the photoemission process has an obvious multiphoton character which has been recognized since the earlier studies.[1] Thus multiphoton photoemission (MPE) shares many features usually encountered in nonlinear processes: For instance, the total photocurrent usually depends on the laser intensity following an Nth power law, where N is the number of photons that have to be absorbed to overcome the surface barrier.[2] Many of these aspects have been investigated by studying the dependence of the total photocurrent on different laser parameters for different types of samples (metals,[3–5] semiconductors,[6,7] or insulators[7–9]); there are fewer studies concerning the energy of the emitted electrons. An early paper,[1] using nanosecond pulses, outlined the importance of the pulse duration, which will be discussed in more detail below. Otherwise, MPE has been recently shown to be a powerful spectroscopic method for the study of surface states, particularly for the case of unoccupied states such as the "image-potential" states.[10] In such studies it is essential to keep the laser intensity as low as possible to avoid any strong perturbation of the state under study. In this case one finds, as expected from a straightforward extension to the case of MPE of Einstein's theory of the photoelectric effect, that the electron energy has a maximum energy of[11]

$$E_e = NE_p - \phi \ , \tag{1}$$

where E_e is the electron energy, E_p the photon energy, and ϕ the work function. This is because only the lowest-order possible process contributes to the emission. The shape of the electron spectrum reflects the density of states in the initial and final states (as in the case of usual photoemission), but also in the intermediate state. Intensity in such experiments usually does not exceed 10^4 W cm^{-2}. In contrast, very-high-intensity experiments (at 10^{13} W cm^{-2} and above, pulse duration in the nanosecond range) have produced very-high-energy electrons (some 10^4 eV and more). In such experiments the sample is usually vaporized, so that it is unclear whether the electrons are accelerated in the laser-surface interaction or in the interaction between the laser and an expanding plasma in front of the surface.

Another outcome of the laser-surface interaction is the emission of heavy particles, ions, or neutrals. This is at the basis of the laser ablation process which has been addressed so far essentially under a practical point of view. How this emission process results from the essential laser-solid interaction, which at visible wavelengths is mediated by the electrons, is a question that has so far been only marginally considered under the fundamental point of view.

As already mentioned, the question of the laser-pulse duration is a major one in such experiments. Indeed, the energy primarily absorbed by the electrons can be redistributed through electron-electron and electron-ion collisions because, unlike in multiphoton experiments in gases, we are dealing here with an extremely condensed medium. The corresponding energy relaxation times are quite short: less than one laser period ($\simeq 10^{-15}$ s) for the electron-electron relaxation time (therefore, this relaxation process is a part of the excitation) and fractions of a picosecond for the "electron-phonon" relaxation time.[12] This is well in the range of what can be achieved nowadays in terms of short laser pulses. The result of an experiment will therefore depend on the laser-pulse dura-

tion in two ways: First, because at a constant intensity the total energy absorbed by the sample is higher when the pulse duration is longer and, second, because in some cases the pulse can be made short enough that the lattice can be considered as "frozen" during the time of the interaction. Early experiments[1] using pulse durations in excess of 10 ns have shown that, in this case, the photocurrent can be due to a thermionic effect of the heating of the sample by the laser pulse. Therefore, all subsequent experiments used picosecond pulses (which allow one to access the same laser intensity with an absorbed energy reduced by a factor 1000). This is the case of the work presented here. Even in this case it was shown that the local and transient heating of the sample could play a significant role in MPE, yielding what was called "thermally assisted" MPE.[13] Some very recent experiments have used laser pulses in the 100-fs range[14] and measured in different ways electron temperatures which are quite high (several 100 000 K), far beyond the solid melting point without damage caused to the surface. Laser intensities used in these experiments are usually quite high ($10^{11}-10^{12}$ W cm^{-2}). Finally, one recent experiment[15] has reported electron energies of 600 eV in a MPE experiment using 8-ps laser pulses at intensities of 25 GW cm^{-2}.

In this work we present results concerning the electron emission by an aluminum surface irradiated by 35-ps pulses at a 532-nm wavelength ($E_p=2.34$ eV), and at 1064 and 355 nm ($E_p=1.17$ and 3.51 eV), and at a somewhat longer pulse duration for comparison purposes. Ion emission is observed using ion-mass time-of-flight spectroscopy. The paper is organized as follows: Section II is a description of the experimental setup and procedures. Section III is a report of the data obtained on ion-mass spectra, intensity dependence of the total photocurrent, and electron energy spectra. In Sec. IV we present a model calculation of MPE using a multiphoton inverse bremsstrahlung picture which we use to estimate the results of a Fowler-Dubridge calculation of the MPE current. All these results are discussed in Sec. V.

II. EXPERIMENTAL SETUP AND PROCEDURES

A. Laser

The laser used in this experiment is a commercial picosecond Nd:YAG system (Quantel). Its output consists of pulses whose duration can be selected between 50 and 135 ps (by a choice of output couplers of different thicknesses). The pulse energy is about 60 mJ, and in most of the experiments we used the shorter pulse duration. The output can be frequency doubled and tripled and is passed, after selection by dichroic mirrors, through a half-wave plate and Glan prism system which is used to adjust and stabilize the laser average energy (within ±5%). Pulse-to-pulse fluctuations are of the order of ±10%. The spatial profile of the laser beam is then restored by severe spatial filtering, and the beam is mildly focused onto the sample surface, at an incidence angle of 75°, usually P polarized. The pulse duration was measured using a streak camera and also checked with an autocorrelator. The irradiated area was determined using the laws of diffraction and the characteristics of our spatial filtering and focusing system. We estimate our uncertainty concerning the laser intensity to about ±30% (a large but usual figure in such experiments), but within a special set of experimental conditions, the precision of the relative intensity measurements is much better (essentially limited by our pulse-to-pulse fluctuations). The laser is operated at a 20-Hz repetition rate. The overall laser system is represented in Fig. 1.

B. Spectrometer

Both ion-mass and electron energy spectroscopy used a time-of-flight spectrometer (Fig. 2), well adapted to experiments where the ion-electron source is pulsed. For ion-mass spectroscopy, the spectrometer was operated in the "reflectron" mode[16] and was specially designed to compensate for high initial kinetic energies (up to several 100 eV) at the expense of the resolution which, in such experiments, does not have to exceed 1/500. For electron energy spectroscopy, the electrons are just allowed to drift freely in a well-shielded field-free region. However, at the input of the spectrometer, a three-grid system is used to secure a proper collection of the electrons. Indeed, as we show hereafter, it is necessary to take care of the space-charge problem, because of the rather high current obtained in this experiment. The three-grid system is shown in the inset in Fig. 2. The first grid can be set to a high positive voltage, setting a high dc field of a few kV cm^{-1} at the sample surface to cancel space charge. The third grid is at the flight tube potential and defines the tube's entrance. Another grid, set at an intermediate potential, is inserted in between those two. It prevents the high reverse field between the two outer grids from leaking inside the flight tube, which causes, in the region of the entrance grid, serious diffraction problems for the lower-energy electrons. Note that this spectrometer has an acceptance angle of 2° when the flight tube is set to the same voltage as the sample. In fact, electrons are usually accelerated by about 2 V before entering the flight tube (the nearly zero-kinetic-energy

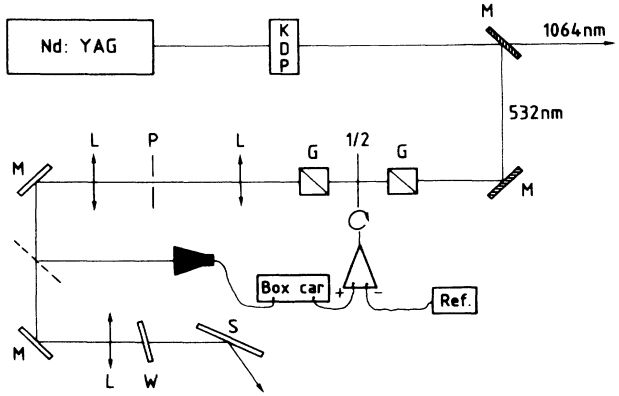

FIG. 1. Laser system layout: M, mirrors; G, Glan prisms; $\frac{1}{2}$, half-wave plate; L, lenses; P, pinhole; W, window; S sample.

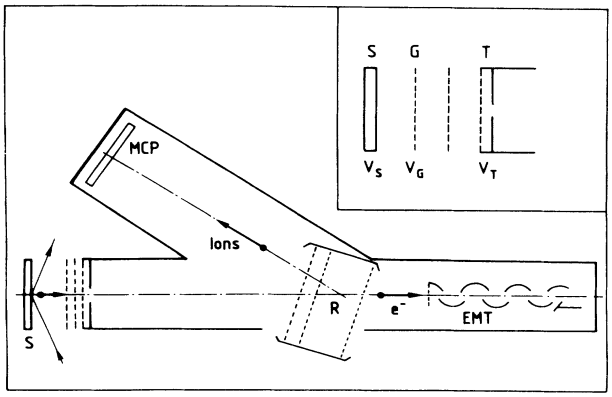

FIG. 2. Electron-energy–ion-mass spectrometer: *R*, ion reflector for operation in the reflectron mode (the inset shows the detail of the input optics); *S*, sample; *G*, extraction grid; *T*, entrance grid (at the flight tube potential).

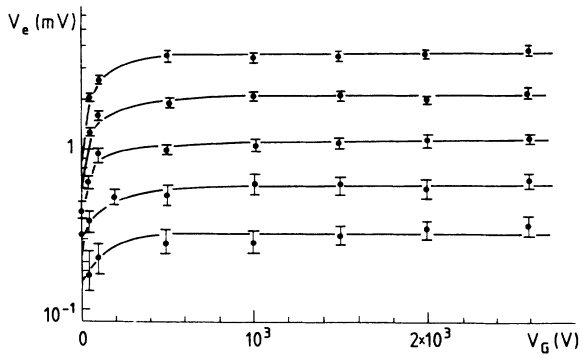

FIG. 3. Dependence of the total photocurrent (measured on the sample) on the extraction grid potential for different laser intensities (increasing from bottom to top). 1500 V corresponds to a field at the sample surface of 1 kV/cm.

electrons would otherwise never reach the detector), and this results in an increase of the acceptance angle. It is a very simple matter to compute this change in the acceptance angle (and thus in the collection efficiency). It depends only on the initial kinetic energy of the electron and potential difference between the sample and flight tube. This is taken into account to correct the electron energy spectra that we present below. The signal from one of the electron multipliers is fed to a sampling oscilloscope (400-MHz bandwidth, 350-MHz sampling rate), averaged over a number of shots, and transferred to a microcomputer in charge of converting the time-of-flight spectra into energy (or mass) spectra. The total photocurrent can be measured with the same oscilloscope plugged directly into the sample polarization circuit.

C. Sample preparation and handling

In this experiment we used a single aluminum crystal cut along its (100) face. The sample was initially prepared by a succession of Ar-ion etching and heating cycles. The surface purity was checked using ion-mass spectrometry of the species desorbed under laser irradiation in a way that will be presented in detail elsewhere. Also, in the course of the experiment, cycles of laser etching and heating were eventually applied. This appears to be a simple and efficient way of restoring the surface cleanliness, instead of ion etching. The sample was maintained in ultrahigh vacuum at a background pressure less than 10^{-10} Torr, and it could be both heated and electrically polarized. We usually worked with the sample at room temperature.

D. Preliminary checks

We first checked our time-of-flight spectrometer by reproducing an experiment whose phenomenology is well documented. Above-threshold-ionization spectra[17] of xenon gas at an intensity around 10^{12} W cm^{-2} were measured. The electron spectrometer energy resolution was found to be about 0.1 eV at 2 eV analysis energy, which is quite sufficient for our experiments. The reflectron mass spectrometer was checked by irradiating a stainless-steel sample at high intensities (in order to produce ions with a high initial kinetic energy) and checking that the ion-mass spectrum was roughly reproducing the sample composition (there is some uncertainty concerning the sputtering rates of the different components). Our apparatus showed the ability of separating the different isotopes of any studied species throughout the whole useful mass range (up to mass 200) for both positive and negative ions.

A crucial problem is that of space charge at the sample surface. Out of the space-charge regime, the total photocurrent should not depend on the extraction field. This dependence is shown in Fig. 3 for different laser intensities. It shows first a steep increase and then a plateau region. All data are reported hereafter have been taken in this plateau region. This was found to be a necessary condition to obtain a dependence of the total photocurrent versus the laser intensity stable with the extraction field. The same measurements were performed for 1.17 and 3.51 eV photon energies to determine in all cases proper (space-charge-free) collection conditions of the electron energy spectra. As in Ref. 15, the electron energy was found to depend on the extraction field and to stabilize at fields much larger than necessary to stabilize the photocurrent. This was considered as the final test for space-charge saturation, and all spectra were therefore recorded using extraction fields of 3 kV/cm or more.

III. EXPERIMENTAL RESULTS

A. Ion-electron yield

Figure 4 shows a positive-ion-mass spectrum taken at a wavelength of 532 nm, a pulse duration of 35 ps, and an intensity of 3×10^8 W cm^{-2}. It consists of one prominent peak at the aluminum mass (27), a few impurity peaks (essentially potassium), which at this intensity form less than 1% of the total spectrum, and a small peak at mass 54, due to Al_2^+ clusters and traces of Al_3^+. A striking feature is that on no occasion were multiply charged Al

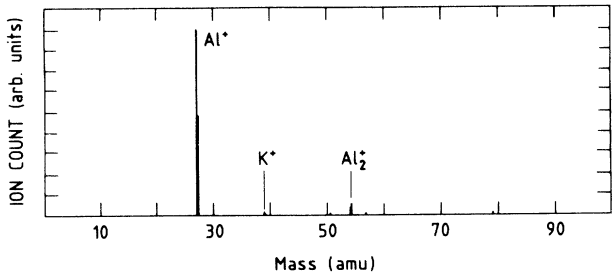

FIG. 4. Typical ion-mass spectrum at an intensity of 0.3 GW cm^{-2}. Such a spectrum is taken after approximately 1 h of sample irradiation. Only K^+ is visible as an impurity on this spectrum. Traces of Na^+ and Cs^+ can be seen at higher intensities.

ions observed, unless the intensity was high enough to produce a surface plasma, easily detected through its light emission: Its uv part would produce a signal at $t=0$ on the electron multiplier, insensitive to any potential in the spectrometer. For the three wavelengths and for two different pulse durations (35 and 95 ps at 532 nm), we measured the number of sputtered aluminum ions as a function of the laser intensity. This was compared to the dependence of the total electron signal (measured as the number of electrons leaving the sample) on the laser intensity. Figures 5(a) and 5(b) show two different cases of such measurements. In case (a) ($E_p=2.34$ eV, $\tau_p=35$ ps), electron emission starts at intensities much lower than ion emission, whereas in case (b) ($E_p=2.34$ eV, $\tau_p=95$ ps), they seem to occur in the same intensity range. It should be kept in mind, however, that the spectrometer's detection efficiency for the ions is of order of one, which is not the case for the electrons (we cannot detect less than 5×10^4 electrons in the total photocurrent measurements). In order to compare the ion and electron yields for different experimental conditions, we need to define a quantity that will not be sensitive to our absolute-intensity measurement. We define the "appearance intensities" for the ion and electron measurements as the intensities at which we measure one ion or 5×10^5 electrons. This yields the different figures listed in Table I, as a function of the laser wavelength and pulse duration. Even if the absolute uncertainty on the laser intensity is quite large (about 30%), it is much less within one special set of experimental conditions. Therefore, the ratios of the intensities in one line of Table I are certainly meaningful quantities (within $\pm10\%$). Note that the electron yield at 2.34 eV shows for both pulse durations a clearly second-order behavior, as expected for a two-photon process ($\phi=4.3$ eV), while the ion emission shows an "intensity-threshold"-like behavior. One can scale the appearance intensity for the electrons down to the one electron level using the intensity dependence of the electron yield measured in Figs. 4(a) and 4(b). It shows that electron emission starts in both cases at much lower intensities than ion emission.

Concerning the orders of nonlinearity (also in Table I), we note that if they agree quite well with the expectations at 2.34 eV, they do not at 3.51 eV (where a second-order process is also expected). At 1.17 eV a slope cannot be

TABLE I. Appearance intensities for detection of 5×10^5 electrons and one ion for different experimental conditions. Experimental orders of nonlinearity for the total photocurrent (K).

E_p (eV)	τ_p (ps)	I_{el}	I_{ion}	K
2.34	35	8.5×10^7	2.3×10^8	2.1
2.34	95	4.2×10^7	3.4×10^7	2.1
1.17	50	2.4×10^8	6.5×10^7	>6
3.51	29	5.2×10^7	2.8×10^8	1.6

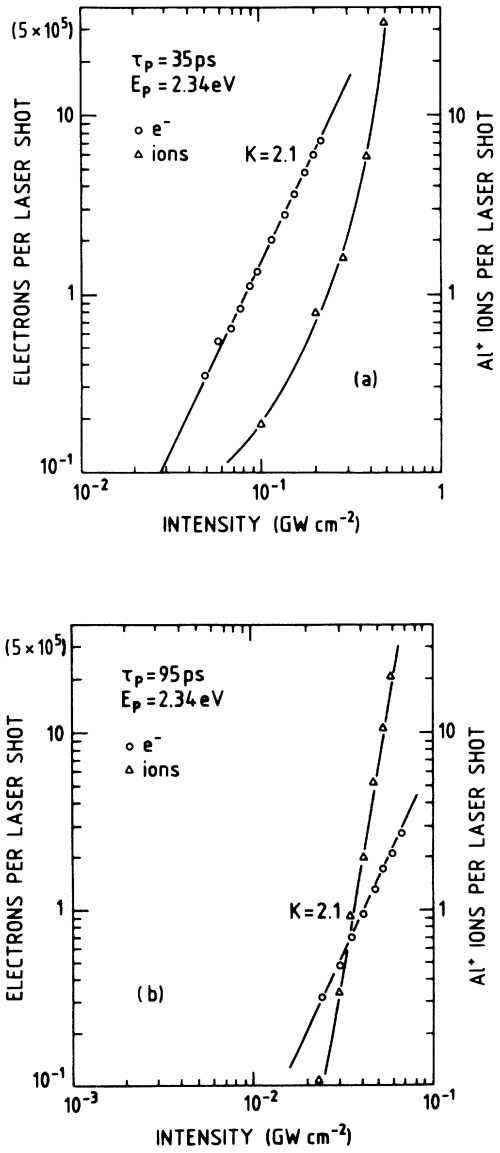

FIG. 5. Total electron signal (circles) and total Al^+-ion signal (triangles) at a 532-nm wavelength for two different laser-pulse durations. Note the shift in the intensity scales between (a) and (b). K is the experimental order of nonlinearity measured as the slope of the electron curve. Lines are drawn through the experimental points.

measured because the photocurrent is found to depend very rapidly on the laser intensity, so that the intensity range over which current measurement are possible is of the order of the intensity error bar. In any case this corresponds to an experimental order of nonlinearity much larger than the expected one (four). At 3.51 eV the discrepancy is in the other direction.

In this experiment it is essential to check that the laser interacts with the surface and not with a plasma expanding in front of it. At higher intensities negative ions can be observed and also an intense light emission. Both are signs of rather dense plasma conditions and are totally absent in the usual conditions of our experiment (as Fig. 4 or for the data presented hereafter). We also searched for a Doppler shift of the light reflected on the sample and could not find any. This indicates that reflection occurs on a motionless surface and not on an expanding plasma, as sometimes has been observed in experiments at higher intensities.[18] All the above observations enable one to define for each set of experimental conditions an intensity range in which electron energy spectra can be collected, being sure that the surface is unaltered, which is the case for all data presented hereafter.

B. Electron energy spectra

Several electron energy spectra (EES) were taken with 2.34 eV photon energy and a 35-ps pulse duration. The laser intensity ranged from the lowest intensity compatible with the overall experimental stability and the "sputtering threshold." Three of such spectra are shown in Fig. 6. They correspond to an average over a few thousand to a few hundred thousand laser shots, depending on the laser intensity. The first spectrum [Fig. 6(a)] was taken at an intensity of 5×10^{6} W cm^{-2} and is essentially compatible with a usual MPE interpretation. The zero energy is directly deduced from the geometrical characteristics of our spectrometer and potentials of the different electrodes and is not corrected from any possible contact potential. If any, it is clearly of small magnitude. The total width of the spectrum is about 1 eV, while a two-photon process at an energy of 2.34 eV yields only a maximum energy of 0.4 eV. Whether this is already the sign of some intensity-induced change in the electron energy or of a change in the work function (due, for instance, to surface contamination) is an open question. However, in view of the spectra of Figs. 6(b) and 6(c), the first interpretation seems the most probable. The spectrum of Fig. 6(b) was taken at an intensity of 3.5×10^{7} W cm^{-2}, and shows a much larger extension toward high energies (up to about 6.5 eV). This goes on with the spectrum of Fig. 6(c), which, for an intensity of 1.2×10^{8} W cm^{-2} shows electrons with energies up to 70 eV. The structures that appear mainly on the spectrum of Fig. 6(b) are not reproducible and are presumably due to statistical fluctuations. When the intensity is further increased, the maximum electron energy keeps increasing, but we enter the "sputtering regime" where the experiment becomes more questionable, though it does not show clearly on the electron spectrum. Results of the same type were obtained at photon energies of 1.17 and 3.51 eV.

In order to clarify the origin of the fast electrons observed in Fig. 6, we recorded a last electron energy spectrum under somewhat different conditions: At the expense of a loss of resolution, the flight tube was set at a 35-eV potential to secure a perfect collection of all the electrons. The spectrum obtained in such conditions (for an intensity of 8×10^{7} W cm^{-2} and a photon energy of 2.34 eV) is shown in Fig. 7. It shows that the spectrum is in fact symmetric around the analysis energy. Its width was found to increase with the extraction field and laser intensity as well (in a way similar to the maximum electron energy in the case of Fig. 6). Note that, when brought back to the sample potential, the low-energy part of the spectrum would correspond to electrons of negative energy. This proves that the cause for the slow electrons in Fig. 7 (and consequently the cause for the fast electrons) cannot be the emission process and has to be sought in transport phenomena.

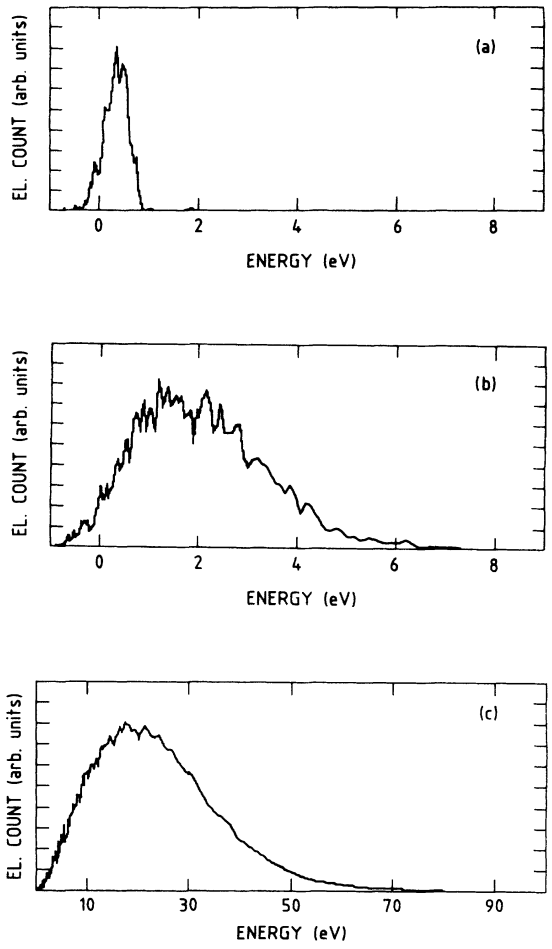

FIG. 6. Three-electron energy spectra taken at three different laser intensities: (a) $I=5\times10^{6}$ W cm^{-2}, (b) $I=3.5\times10^{7}$ W cm^{-2}, and (c) $I=1.2\times10^{8}$ W cm^{-2}. No correction is applied to account for an eventual contact potential. Note the 10× scale contraction in (c).

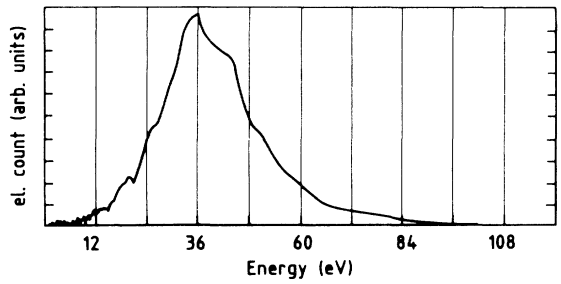

FIG. 7. Electron energy spectrum obtained with the analysis energy set at 35 eV, showing a symmetric broadening of the spectrum. $E_{ex}=3\times10^3$ V/cm, $E_p=2.34$ eV, and $I_1=8\times10^7$ W cm^{-2}.

IV. THEORETICAL ESTIMATE OF THE MPE CROSS SECTIONS

Despite the importance of photoemission as a spectroscopic tool, there are very few exact calculations of photoemission cross sections, even in the linear case [interpretation of ultraviolet photoemission spectroscopy (UPS) or x-ray photoemission spectroscopy (XPS) spectra usually relies simply on the identification of spectral features with structures in the density of states, little attention being paid to the exact amplitude of the photoemission cross section]. Extension of one-photon photoemission calculations to the multiphoton case is well beyond the scope of this paper, even though this problem is worth tackling. We are here mostly interested in the respective orders of magnitude of the MPE cross sections of different orders. In this respect we can take advantage of the fact that the laser essentially interacts with electrons with an energy close to the Fermi energy (within one-photon energy), which in the case of aluminum are very close to free electrons. We thus consider the problem of scattering a free electron on a localized potential in the presence of the laser field. The potential can be an impurity, a step potential, or a muffin-tin approximation of the ion potential. The electron states are represented by plane waves. The differential cross section of multiphoton inverse bremsstrahlung for electrons scattered in the direction of the laser polarization is computed using the Kroll-Watson formula[19] (which requires the use of the first Born approximation). They were averaged over the initial distribution of electron momentum, assumed to be isotropic. The potentials used in the three cases were of the type

$$U(r)=-U_0\frac{e^{-r/a}}{r} \tag{2}$$

(a Yukawa potential; U_0 and a are, respectively, the amplitude and range of the potential) in the case of an impurity, and the initial state is taken as a plane wave with the Fermi energy,

$$U(r)=-\frac{U_0}{1+e^{x/a}}\ , \tag{3}$$

for the step potential; the initial state is a plane wave with the energy corresponding to the absorption of two photons by a Fermi electron. The potential is taken numerically from the tables of Moruzzi, Janak, and Williams[20] in the case of the muffin-tin potential, and the initial state is the same as in the case of the Yukawa potential. The resulting probabilities for different orders are given in Table II (for $a=5$ Å), at a field amplitude of 10^8 V/m (intensity of 6.6×10^8 W cm^{-2}). It shows that, in the three cases, the cross section is small and that it decreases very fast with the order of the process. This is nothing but what was expected, because the intensity is obviously not high enough to jeopardize the convergence of the perturbation series. There are many approximations in this calculation. The range of the potential in the first two cases is somewhat arbitrary. The probability increases with the range ($\partial V/\partial\tau$ is smaller, but the electron feels the potential longer) particularly at small orders, and in this respect 5 Å is already a large value. Second, the step potential we have used is a loose approximation for the surface potential. Finally, the first Born approximation is valid at electron energies large compared to the depth of the potential, which is not really the case here. We checked, by changing the initial energy, the influence of this approximation, and the result is that the cross section does change, but by no more than three orders of magnitude in the case of a ten-photon absorption. Concerning the scaling of the cross section with the laser intensity, though this calculation is nonperturbative, it strictly fits a perturbative dependence (I^k for a kth-order process). A key result of the calculation (which is, in fact, built in the Kroll-Watson formalism) is that though the absolute cross sections depend on the specific potential, the *ratios of the cross sections of different orders for the same potential do not.* Table II thus shows that even if photoemission, for energy-conservation reasons, is of the second order, the *laser-electron coupling is essentially dominated (by about four orders of magnitude) by the linear, single-photon interaction.*

The cross sections of Table II do not represent the whole photoemission process. One has to account for the escape probability of the electron (once it has been excited above the vacuum level) and of the changes presum-

TABLE II. Cross sections (in atomic units) for inelastic scattering along the laser polarization with absorption of N laser photons on (1) a Yukawa potential and (2) a step potential.

Potential	Range (Å)	$N=1$	$N=2$	$N=5$	$N=10$
(1)	5	0.45×10^{-4}	0.85×10^{-9}	0.94×10^{-22}	0.34×10^{-45}
(2)	5	0.72×10^{-7}	0.85×10^{-12}	0.13×10^{-26}	0.30×10^{-52}
(3)	2.8	0.40×10^{0}	0.49×10^{-4}	0.75×10^{-17}	0.30×10^{-40}

ably caused by the laser-induced heating of the sample to the initial distribution of states. This is properly done in the Fowler-Dubridge theory of photoemission.[4,11] The physics underlying this theory is rather simple: The absorbed fraction of the laser energy induces an increase of the sample temperature. The Fermi distribution thus extends toward high energies, so that emission through absorption of less photons may become possible. The photocurrent is then a sum of photocurrents of different orders:

$$J=\sum_{n=0}^{\infty} J_n \ , \tag{4}$$

where n represents the number of photons absorbed, and with

$$J_n(I,T)=C_n(e/E_p)^n A I^n (1-R)^n T^2 F\left[\frac{E_p-\phi}{kT}\right] . \tag{5}$$

In Eq. (5), I is the laser intensity at the surface, R the surface reflection coefficient [so that $(1-R)I$ represents the intensity inside the sample], A the theoretical Richardson coefficient (120 Å/cm^2 K^2), and F is the Fowler function:

$$F(x)=\begin{cases} \displaystyle\sum_{m=1}^{\infty} (-1)^{m+1} e^{mx}/m^2, & x\le 0 \\ \pi^2/6+x^2/2+\displaystyle\sum_{m=1}^{\infty} (-1)^{m+1} e^{-mx}/m^2, & x>0 \ . \end{cases} \tag{6}$$

In the temperature range of interest here, the expansion is essentially dominated by the first term. For electron energies above the vacuum limit, F is essentially constant, whereas it has an exponential behavior with the temperature for electrons below the vacuum limit. C_n is a coefficient which contains both the multiphoton absorption cross section and the escape probability of the electron. The scattering cross sections computed in Table II are, in fact, very close to the quantity $C_n I^n (1-R)^n$. Usually, the C_n's are used as experimental parameters and adjusted to fit the data. In the following discussion, we will use the opposite point of view: We will admit that since the electrons we detect are released in similar conditions of energy, in the same region of the sample, their escape probabilities are of the same order of magnitude and, therefore, that the amplitude of the C_n's is essentially determined by that of the absorption cross section. If one is interested in the ratios of processes of different orders, this is certainly a reasonable assumption, which allows to use cross sections such as those of Table II for quantitative estimates.

V. DISCUSSION

A first question which has to be settled is that of the fast electrons observed in this experiment (Fig. 6) and in several others in similar conditions. The production of "hot" electrons in laser-matter interaction is not a new observation *per se,* even in quite elementary processes such as multiphoton ionization in a dilute gas phase. It is known that the process of above-threshold ionization (ATI), because of multiphoton transitions in the ionization continuum of an atom, can produce rather high-kinetic-energy electrons.[11] However, such processes are observed at intensities four to five orders of magnitude higher than the ones used in this experiment [multiphonon ionization (MPI) of xenon by 1.17-eV photons yields electrons with energies up to 15 eV at a laser intensity of about 10^{13} W cm^{-2}], so that such an explanation does not seem probable. The calculations of Sec. IV confirm this conclusion, as does the fact that no multiply charged ions are detected. Local thermal equilibrium involving 70-eV electrons would result in ions with ionization stages up to 4. Such an equilibrium is likely to be reached since our pulse duration is still a few orders of magnitude higher than the longer energy-relaxation-time constants of the problem (electron-phonon relaxation time $\simeq 10^{-13}$ s). Another suggested origin for these high-energy electrons was surface plasmon relaxation,[21] quite unlikely in our case: We are very far from a resonant coupling because of the low energy of our photons compared to the Al plasmon energy and because of the impossibility of coupling surface plasmons to the laser field in the case of a polished surface. A number of recent works on the physics of the transport of electron bunches in high static electric fields,[22,23] confirmed by a careful modeling of our experimental conditions, which will be presented elsewhere, lead to the conclusion that the energy is gained by the electrons during their transport to the detector and not in the interaction. This is consistent with the observation of Fig. 7 of a symmetric broadening of the electron spectrum. As a consequence, we conclude that, as shown by the dependence of the photocurrent on the laser intensity, the photoemission process is dominated by the lowest possible order, namely, the second order in the case of 2.34 eV electron energy.

The high order of nonlinearity measured at 1064 nm is further evidence of this. The paradox contained in this statement is easily solved in the framework of the Fowler-Dubridge theory of photoemission. We assume for simplicity that the sample temperature grows linearly with the laser intensity (no noticeable heat flow in the sample during the pulse duration). This allows one to estimate the temperature increase of the sample, simply obtained from the specific heat of aluminum, and the magnitude of the absorbed energy, yielding 500 K at a laser intensity of 10^8 W cm^{-2}. The difference in the results obtained at 1.17 and 2.34 eV is then easily understood: The third-order, thermally assisted, photocurrent dominates in the 1.17-eV case, whereas the usual second-order process does at 2.34 eV. This is the result of two different effects: First, these results are obtained at different laser intensities, respectively around 0.25 and 0.075 GW cm^{-2}, so that the sample temperature is higher in the 1.17-eV case. Second, the absorption cross section has to make up for a 35 (respectively 10) orders of magnitude difference between the temperature-dependent coefficients in the 2.34-eV case, and only 15 (respectively 5) orders of magnitudes in the 1.17-eV case at a temperature of 300 K (respectively 1000 K). In comparison, the ratio of the ab-

sorption cross sections involved, computed from the conditions of Table II, is

$$\sigma_4/\sigma_3 = 6.5\times10^{-4} \text{ at } 1.17 \text{ eV},$$
$$\sigma_2/\sigma_1 = 1.2\times10^{-4} \text{ at } 2.34 \text{ eV},$$
$$\sigma_2/\sigma_1 = 2.5\times10^{-5} \text{ at } 3.51 \text{ eV},$$

and we recall that these ratios are not potential dependent. Consequently, not only does the temperature favor the third-order process compared to the fourth-order one, in the case of 1.17 eV, when compared to the other cases, but also the ratio of the absorption cross sections. This may partly explain the result at a 3.51 eV photon energy, to which only the first effect applies [only 16 (respectively 6) orders of magnitudes separates the temperature-dependent coefficients for the one- and two-photon processes in this case]. The intensity is at 3.51 eV of the same order as in the 2.34-eV case, and one could admit that this is the dominant factor, but one would in this case expect a similar dependence in both cases. The lower experimental order of nonlinearity at 3.51 eV cannot be explained in the framework of the Fowler-Dubridge theory except through an unusual intensity dependence of the absorption cross section. This point clearly deserves further studies.

Ion (and neutral) emission is generally believed in the case of metals to be essentially a thermal process. The energy absorbed by the electrons is transferred to the lattice via electron-phonon relaxation. This energy is essentially dumped into the metal over a time scale of the order of the pulse duration, whereas heat diffusion operates on longer time scales. Therefore, thermalization of this energy produces an instantaneous increase of the lattice temperature which can reach the metal melting point. The data presented above brings a few indications: We have already noted that the sample instantaneous temperature is probably higher at 1.17 eV than at the other photon energies, which is confirmed by the appearance intensities measurements of Table I. Concerning the intensity dependence of the ion current, one expects it to be dominated by the linear absorption of light (as shown in Table II), as generally observed in laser ablation experiments (where the ablated mass increases linearly with the laser fluence). This is also indicated by the fact that the appearance intensity shows little dependence with the photon energy (the remaining dependence may simply come from the shortening of the pulse duration that results from frequency doubling or tripling). The dependence of the appearance intensity on the pulse duration at 2.34 eV is a little larger than expected, but still within our experimental error bar on the absolute intensity measurements. All this leads to the conclusion that the laser fluence is indeed the essential parameter as far as "heavy"-particle emission is concerned. However, the number of detected ions certainly does not depend linearly on the laser intensity. The "threshold behavior" that can be observed in Fig. 5 may be explained by the fact that ion formation is a process more complicated than the simple sputtering of a neutral atom: It will, for instance, require a collision between a neutral and an excited electron and, thus, should depend more strongly on the laser intensity than the simple neutral emission.

VI. CONCLUSION

Electron and ion emission by an aluminum surface submitted to moderate laser irradiation in the picosecond time regime have been studied. Electron emission strongly dominates at low intensity. The intensity dependence of the total photocurrent can be accounted for by a two-photon process at 2.34 eV photon energy and by a thermally assisted four-photon process at 1.17 eV. This is consistent with the fact that comparison of the electron and ion current indicates a higher instantaneous sample temperature in the latter case. At 3.51 eV the order of nonlinearity measured is lower than the expected value, a point for which there is not definite explanation. Al ions measured are singly charged ions, unless one gets into the surface plasma regime. These results agree on the whole with a multiphoton interpretation for electron emission and a thermally initiated process concerning ion emission.

Electron energy spectra reveal surprisingly high energies given the moderate intensities at which this is observed. The idea sometimes found in the literature that above-threshold photoemission would occur in a very different manner in solids does not resist a calculation of the cross sections which, despite a few approximations, certainly gives the right order of magnitude for the absorption of many photons by the aluminum quasifree electrons. Moreover, the order of nonlinearity of the total photocurrent suggests that emission is due to a two-photon process. Finally, comparison of the electron energies with the ionization energies of the ions detected would suggest a strong deviation from local thermal equilibrium, which is rather unlikely. We have shown that the observation of fast electrons is correlated with that of slow electrons; in other words, that the broadening of the electron energy spectrum is in fact symmetric. This effect that can be explained by modeling the transport of emitted electrons in the spectrometer. A serious question is then to decide whether any electron energy measurements are possible at such laser intensities. A solution to this problem is to reduce the number of electrons emitted at a given laser intensity. This can, for instance, be achieved by using subpicosecond pulses. This solution also offers an opportunity to minimize thermal effects which are still detectable in some of the experiments we have presented.

ACKNOWLEDGMENTS

The authors want to thank Dr. C. Boiziau, Dr. M. C. Desjonqueres, Dr. R. R. Freeman, Dr. J. Friedel, Dr. J. Kupersztych, Dr. C. Manus, Dr. A. Maquet, Dr. Ph. Nozières, and Dr. D. Spanjaard for numerous and fruitful discussions. They also want to acknowledge the technical assistance of M. Bougeard and J. C. Molinari.

[1]E. M. Logothetis and P. L. Hartman, Phys. Rev. **187**, 460 (1969).
[2]Gy. Farkas, in *Multiphoton Processes,* edited by J. H. Eberly and P. Lambropoulos (Wiley, New York, 1978), pp. 81–100.
[3]Gy. Farkas and Z. Gy. Horvàth, Opt. Commun. **12**, 392 (1974).
[4]J. H. Bechtel, W. L. Smith, and N. Bloembergen, Opt. Commun. **13**, 56 (1975); Phys. Rev. B **15**, 4557 (1977).
[5]L. A. Lompre, J. Thebault, and Gy. Farkas, Appl. Phys. Lett. **6**, 110 (1975).
[6]M. Bensoussan and J. M. Moison, Phys. Rev. B **27**, 5192 (1983).
[7]W. J. Sieckhaus, J. H. Kinney, D. Milam, and L. L. Chase, Appl. Phys. A **39**, 163 (1986).
[8]G. Petite, P. Agostini, C. Boiziau, J. P. Vigouroux, C. Le Gressus, and J. P. Duraud, Opt. Commun. **53**, 189 (1985).
[9]E. Matthias, H. B. Nielsen, J. Reif, A. Rosen, and E. Westin, J. Vac. Sci. Technol. B **5**, 1415 (1987).
[10]W. Steinmann, Appl. Phys. A **49**, 365 (1989).
[11]P. Agostini and G. Petite, Contemp. Phys. **29**, 57 (1988).
[12]R. W. Schoenlein, W. Z. Lin, J. G. Fujimoto, and G. L. Easley, Phys. Rev. Lett. **58**, 1680 (1987).
[13]R. Yen, J. Liu, and N. Bloembergen, Opt. Commun. **35**, 277 (1980).
[14]H. M. Milchberg, R. R. Freeman, S. C. Davey, and R. M. More, Phys. Rev. Lett. **61**, 2364 (1988).
[15]Gy. Farkas and Cs. Toth, Phys. Rev. A **41**, 4123 (1990).
[16]B. Mamyrin, V. Kataraev, and V. Shmikk, Zh. Eksp. Teor. Fiz. **64**, 82 (1973) [Sov. Phys. JETP **37**, 45 (1973)].
[17]P. Agostini, F. Fabre, and G. Petite, in *Multiphoton Ionisation of Atoms,* edited by S. L. Chin (Academic, Toronto, 1984), pp 133–153.
[18]M. Milchberg and R. R. Freeman, Phys. Rev. A **41**, 2211 (1990).
[19]N. M. Kroll and K. M. Watson, Phys. Rev. A **8**, 804 (1973).
[20]V. L. Moruzzi, J. F. Janak, and A. R. Williams, *Calculated Electronic Properties of Metals* (Pergamon, New York, 1983).
[21]T. Tsang, T. Srinivasan-Rao, and J. Fisher, Phys. Rev. B **43**, 8870 (1991).
[22]U. Kolac, M. Donath, K. Ertl, H. Liebl, and V. Dose, Rev. Sci. Instrum. **59**, 1933 (1988); R. Azria, J. P. Ziesel, P. Girard, J. P. Guillotin, and Y. Le Coat (private communication).
[23]H. J. Drouin and Ph. Brechet, Appl. Phys. Lett. **56**, 2152 (1990); see also J. P. Girardeau-Montaut and C. Girardeau-Montaut, J. Appl. Phys. **65**, 2889 (1989), Phys. Rev. A **44**, 1409 (1991).